

ВЗАИМОСВЯЗИ МЕЖДУ НЕОДНОРОДНОСТЬЮ РАСПРЕДЕЛЕНИЯ МЕХАНИЧЕСКИХ СВОЙСТВ УГЛЕЙ НА МИКРО- И НАНОУРОВНЯХ И ИХ СПОСОБНОСТЬЮ К ВНЕЗАПНЫМ ВЫБРОСАМ И РАЗРУШЕНИЮ

Е.Л. Коссович¹, С.А. Эпштейн¹, Ф.М. Бородич², Н.Н. Добрякова¹, В.А. Просина¹

¹ НИТУ «МИСиС», Москва, Россия, e-mail: e.kossovich@misis.ru

² Университет Кардиффа, Кардифф, Великобритания

Аннотация: Внезапные выбросы угля и газа являются одними из наиболее опасных явлений при добыче угля. В связи с этим изучение природы этих процессов является приоритетным для угольной промышленности. В настоящей работе показано, что особенности структуры витринита каменных углей на микро- и наноуровне в значительной степени определяют их склонность к внезапным выбросам и образованию тонкодисперсных частиц. В качестве объектов исследования выбраны угли из разных пачек одного пласта, различающихся по потенциальной выбросоопасности. Для работ использовали аншлиф-брикеты исходных углей и углей, подвергнутых сорбции в среде диметилформамида. Показано, что способность углей к разрушению и образованию тонкодисперсных частиц при механическом одноосном нагружении (микроиндентировании) находится во взаимосвязи с распределением их механических свойств и дефектов, построенным по результатам автоматизированного микроиндентирования по сетке на площадках, размеры которых сопоставимы с размерами контактов между поверхностью образца и иглой микроиндентора. Обнаружено отсутствие взаимосвязи между особенностями структуры витринита углей из потенциально опасной и неопасной пачек и средними величинами твердости, а также ее распределением по поверхности образцов. Установлено, что для угля из потенциально выбросоопасной пачки характерна более высокая неоднородность распределения величин модуля упругости (как характеристики «жесткости» материала — способности к сопротивлению деформированию) по сравнению с углем из неопасной пачки. Сопоставление полученных результатов с данными об образовании трещин в области контакта при микроиндентировании позволяет сделать вывод о существовании тесной взаимосвязи между высокой неоднородностью распределения «жесткости» витринита углей из потенциально выбросоопасных пачек с их способностью к разрушению при механическом нагружении. Для оценки способности углей к образованию тонкодисперсных частиц при механических воздействиях был использован параметр RW , вычисляемый на основе анализа диаграмм «нагружение-глубина внедрения» как отношение работы, потраченной на необратимые изменения в структуре материала, в полной работе по вдавлению при микроиндентировании. Обнаружено, что образцы угля из неопасной пачки характеризуются низким количеством включений (областей на поверхности), склонных к необратимым изменениям структуры, по сравнению с включениями, способными сохранять структурную целостность. Для углей из потенциально выбросоопасной пачки характерно равное соотношение таких включений. Сорбционное взаимодействие углей с диметилформамидом позволило частично снять внутренние напряжения, существующие в их структуре. Это дало возможность выявить различия в механических свойствах двух исследованных углей, обусловленные особенно

стями структуры витринита. Представленные в работе результаты показали, что анализ распределения механических свойств по данным наноиндентирования позволяет качественно и количественно выявлять способность углей к разрушению и внезапным выбросам.

Ключевые слова: уголь, механические свойства, неоднородность, тонкодисперсная пыль, хрупкость, сорбционное разупрочнение.

Благодарность: Работа выполнена при поддержке Российского научного фонда (грант № 18-77-10052).

Для цитирования: Коссович Е. Л., Эпштейн С. А., Бородич Ф. М., Добрякова Н. Н., Просина В. А. Взаимосвязи между неоднородностью распределения механических свойств углей на микро- и наноуровнях и их способностью к внезапным выбросам и разрушению // Горный информационно-аналитический бюллетень. – 2019. – № 5. – С. 156–172. DOI: 10.25018/0236-1493-2019-05-0-156-172.

Connections between micro/nano scale heterogeneity of mechanical properties of coals and their propensity to outbursts and crushing

E.L. Kossovich¹, S.A. Epshtein¹, F.M. Borodich², N.N. Dobryakova¹, V.A. Prosina¹

¹ National University of Science and Technology «MISIS», Moscow, Russia, e-mail: e.kossovich@misis.ru

² Cardiff University, Cardiff, UK

Abstract: The outbursts of coal and gas is one of the main coal mining hazards, therefore, for the coal mining industry, studying of mechanisms and predisposing factors for these events is of the utmost importance. It is demonstrated here that the micro/nano scale structure of coal samples is one of predisposing factors for the coal propensity to outburst. The same is related to the coal propensity to crushing and formation of fine powder (dust). The results of micro/nanoindentation experimental studies of heterogeneity of spatial distribution brittleness and mechanical properties of coals at micro/nano scales are presented for samples taken from both hazardous (outburst-prone) and non-hazardous strata (packs) of the same coal seam. The experiments were performed on both 'as received' coal samples and ones after sorption treatment by dimethylformamide. The latter treatment allowed to partially discharge the internal stresses that exist in the coal samples. The mapping the indentation results enabled us to reveal the actual heterogeneity of distribution of mechanical properties at nanoscale. It has been confirmed that hardness of coals at micro- and nanoscale is not an informative parameter for characterization of their propensity to destruction. It was established that higher heterogeneity of stiffness could be a reason to formation of multiple cracks at coals after microhardness tests. The part of energy spent for the irreversible changes in the material structure within the total work of indentation is the parameter indicating clearly the propensity of coal samples to crushing and formation of fine powder (dust). Coal samples from the non-hazardous packs have a low ratio of inclusions prone to irreversible changes of the structure and those prone to keeping their structural integrity, while the ratio is about a unity for samples from the hazardous packs. Thus, there is a natural distinction of the mechanical properties between two coal samples having similar origin and rank but different in their proneness to instantaneous outbursts.

Key words: coal, mechanical properties, heterogeneity, fine dust, brittleness, sorption-induced strength degradation

Acknowledgements: This work was supported by the Russian Science Foundation (grant # 18-77-10052).

For citation: Kossovich E. L., Epshtein S. A., Borodich F. M., Dobryakova N. N., Prosina V. A. Connections between micro/nano scale heterogeneity of mechanical properties of coals and their propensity to outbursts and crushing. *Gornyy informatsionno-analiticheskiy byulleten'*. 2019;5:156-172. [In Russ]. DOI: 10.25018/0236-1493-2019-05-0-156-172.

Introduction

Sudden ejections of very fine coal dust and gas from a seam could occur at any time during open and underground mining. Being spontaneous and, in some cases, lasting for a considerable timespan, this outburst phenomenon may release up to several tons of coal dust mixed with explosive gas [1–4]. This may lead not only to losses of the mining equipment, but it can also cause fatalities [4]. The coal dust itself is a significant threat both to the safety of people and to the environment [1, 2]. The fine coal dust can also appear during mining, storage, transportation and processing of coals. The coal dust particles whose sizes are less than 10–25 μm [5,6] are especially dangerous as the dust is able to stay in the air for a long period of time [7]. It is argued in [7] that the span of dangerous sizes of coal particles should be extended up to 75 μm . Because the aerosol dust can be transported in the air for rather long distances, the areas outside the sanitary protective zones of enterprises and cargo ports may be also affected by negative impacts of coal dust [2].

As predisposing factors for the outburst phenomena, the following reasons are pointed out in the literature: stress conditions and tectonics, geological conditions, gas stored inside the coal matter, some other structural and mechanical properties of coal (see, e.g. [3, 4, 8–11]). Mainly the related papers consider coal as a rather homogenous material and provide the results on the mechanical fracturing tests at large scales [12]. These studies concentrated mainly at coals propensity to fracture under external and internal (caused by internal gas flow) stresses [13]. There are just few papers reported on high effects of coals microstructure (macerals composition) on outbursts hazards [14–16]. However, it has been recently shown that coals vitrinite structural heterogeneity

has a vast impact on the coal propensity to outburst [17].

The aim of this paper is to demonstrate that the spatial heterogeneity of micro/nano scale mechanical properties of coal components, namely, the components of the vitrinite macerals group, is correlated with the propensity of coals to outbursts and crushing, and in turn to coal dust formation. The heterogeneity of mechanical properties of coals includes the variation in elastic moduli, hardness and other mechanical characteristics at nanoscale. The heterogeneity causes the initiation and further development of fractures and partitioning of coal samples. To justify this assumption, it was proposed to perform a set of experimental studies that include a grid nanoindentation of vitrinite regions of coal samples along with further analysis of the obtained maps of distributions of the mechanical properties. The samples were taken from the same coal seam; they have the similar rank; however they differ because they were taken from hazardous (outburst-prone) and non-hazardous strata (packs).

Materials and Methods

Samples selection and characterization

Two hard coal samples originated from Vorkuta coalfield (Vorkutinskaya mine) were taken for the studies. As it has been mentioned above, these samples are from the same seam, but they belong to packs that differ by the outburst hazard degree: the coal #1 from lower pack (it was not prone to outbursts); and the coal #2 originates from an outburst-prone section of the upper pack. The coal #2 is characterized by relatively higher value of vitrinite reflectance index ($R_{o,r} = 0.924\% \text{Vol.}$) in comparison with the coal #1 ($R_{o,r} = 0.885\% \text{Vol.}$) [17]. According to [17], the packs of the coals #1 and #2 were related to different genetic types with respect to vitrinite reduction (including the degree of hetero-

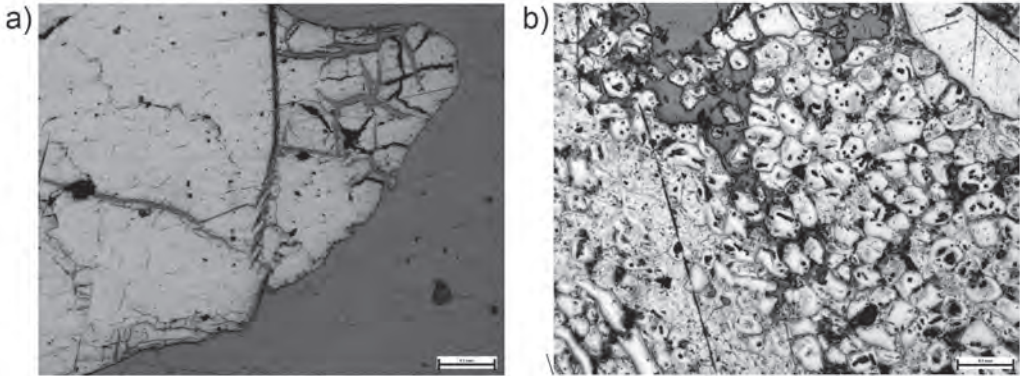


Fig. 1. Surface of the considered coal samples after dimethylformamide treatment: the coal #1 of IV genetic type taken from the non-hazardous pack (a); the coal #2 of II genetic type with respect to vitrinite reduction taken from outburst-prone pack (after [17]) (b)

genicity of internal vitrinite structure): the coal #1 was referred to IV genetic type (optically homogenous), whereas the sample originated from the pack potentially prone to outbursts was related to II genetic type (heterogenous vitrinite structure).

For further features of sorption-induced strength decay of these coals, we address the reader to the results presented in [17]. Sorption-based impacts at these coals also lead to rather different surface degradation (destruction). The interaction with dimethylformamide of the coal #1 having a rather homogenous structure of vitrinite, led to a clear visibility on the sample surface of a grid-like net of relatively straight fractures with pronounced directions of propagation (see Fig. 1, a). The interaction with dimethylformamide of the coal #2 having a highly heterogenous structure of vitrinite, led to drastic alteration of its surface with formation of chips and fractures without any ordered fracture pattern (Fig. 1, b).

It is worth to mention that the sorption treatment of the coals led to significant changes of their supramolecular structure. This, in turn, could possibly lead to partial discharge of the residual stresses that are usually being found in coals matter. On the other hand, the residual stresses may

highly affect the measured mechanical properties and the experimental force-displacement ($P-h$) curves of nanoindentation tests [18, 19], hence we can assume that the sorption treatment enabled us to study the natural heterogeneity of mechanical properties of coals that are not affected by the residual stresses.

In the current studies, for each of the coals, two types of samples were prepared: (i) 'as received' and (ii) 'treated by dimethylformamide'. First, the coal particles whose sizes were in the range of 3–5 mm were taken from each of the packs. Then metallographic specimens were prepared from the particles [20]. The micro- and nanoindentation tests were performed using regions of vitrinite maceral group of these specimens. Vitrinite was selected for the tests because it reflects the principal mechanical properties of coals [21]. Actually, if a coal is considered as a natural organic composite material, then this maceral may be treated as the matrix of the composite [22]. Because the sorption treatment revealed a number of fractures of sample vitrinite surfaces, the micro- and nanoindentation tests of the samples were performed on undamaged regions in order to avoid possible errors in measurements due to the neighboring fractures.

Micro- and nanoindentation techniques

Microhardness tests were performed in accordance with the standard techniques [23, 24]. PMT-3 device [25] was used accompanied by MMS 'Microhardness' software and video camera for obtaining the images of the resulting imprints and evaluation of microhardness. The load applied to the indenter was 200 mN. Sets of indentation tests of vitrinite maceral group were performed (each set involved not less than 30 indents). After each indentation test, the shape of the remaining imprint was analyzed for the presence of different types of fractures. The results of microhardness tests have been already described in [17] and they are not repeated here.

Nanoindentation experiments were performed at Hysitron TI 750 instrumental indentation setup. The experimental procedure was fully described in [21, 26]. Tests were performed at homogenous regions occupied by vitrinite macerals group. At least two regions were selected at each sample. Automated grid indentation procedure was applied at zones of 50x50 microns, there were not less than 36 indents at each of the selected zones. The distance between the indents was not less than 8 μm .

Elastic contact moduli (E , GPa) and hardness values (H , MPa) were measured. Also, a statistical parameter R was calculated for each of the indentation experiments. This parameter was used in [21, 26] as a measure of the irreversible changes in coals matter after mechanical impacts. The characteristics of these parameters regarding their meaning are described below in the next section. Further, automatic grid processing was done using MS Excel software and maps describing the mechanical properties variations at the selected regions were plotted for each of the experiment.

Physical meanings of the nanoindentation parameters and interpretation

The depth-sensing indentation techniques mean that both the external load (P) and the displacement of the indenter (h) are continuously recorded. The unloading branch of the 'load-depth of indentation' curve is usually used to evaluate the contact modulus of the sample. A typical shape of the $P-h$ curve is shown in Fig. 2 for the 'as received' sample of the coal #1. It is worth mentioning that the full $P-h$ curve contains a large amount of information on the materials response to the

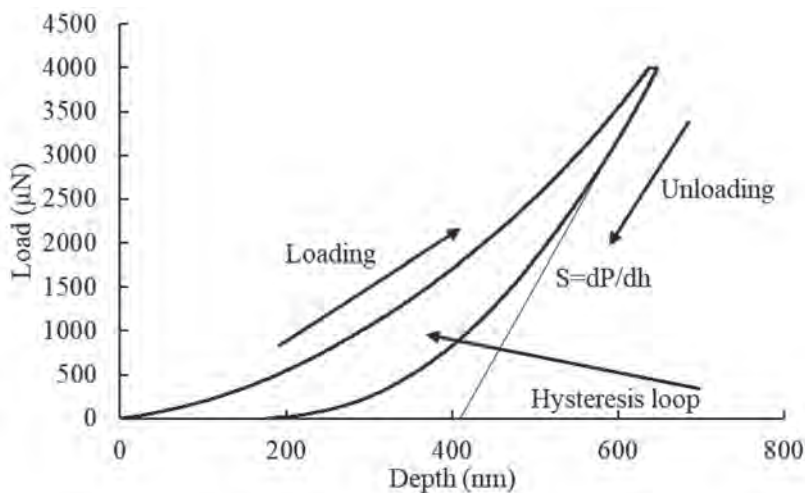


Fig. 2. Typical $P-h$ curve obtained by indentation of the 'as received' sample of the coal #1

external mechanical actions. Typically, the $P-h$ curve contains two branches, where the former describes the loading, and the later describes the unloading processes. These branches usually do not coincide forming the so-called hysteresis loop. The latter shows the existence of the dissipated energy that has led to the irreversible changes of the material structure (plastic deformation). On the other hand, brittle materials also appear to have a hysteresis loop. In this case, it is referred to brittle crushing of material under the applied load either on the sample surface or beneath the surface [27].

Recently, it has been shown that coals tend to crush during depth-sensing indentation [26, 28]. Let us remind that the parameter R_w was introduced [21, 26] as a ratio of the hysteresis loop area (the energy that was spent on irreversible deformations in the material) to the total loading work (the total area below the loading branch of the $P-h$ curve). It is worth mentioning that R_w parameter is the quantity that could be directly measured by the experiments. This ratio could be treated as a share of work that was introduced for the irreversible changes in the material structure in the total work used for its deformation. Because this parameter is tightly connected with the hysteresis loop, for brittle materials it could be treated as a quantitative measure for coals propensity to crushing: the higher is the value of R_w , the more the material is prone to degradation and formation of fine powder in the region of its contact with indenter tip.

Other values, such as the elastic contact modulus and hardness, may be evaluated in accordance with a more advanced analysis of the $P-h$ curves. The elastic contact modulus is connected to the materials stiffness [29, 30], i.e. the materials resistance to deformations. Similar meaning has hardness, which is a measure of the resistance to plastic deformations. It

has been shown recently that coals hardness should not be considered as the material constant because coals may crush into fine powder at indentation loading [26, 28]. Therefore, one should be especially careful when discussing the micro- and nanohardness of coals measured by the standard techniques.

The consequence of formulae for determination of the elastic modulus is as follows. In 1975 the Bulychev-Alekhin-Shorshorov relation (BASH) relation was derived [31]

$$S = dP / dh = 2E^* a \approx 2E^* \sqrt{A / \pi} \quad (1)$$

where S is the stiffness or the inclination of the displacement-load curve (see Fig. 2), a is the characteristic size of the contact zone, A is the area of the contact region and E^* is the contact (reduced) elastic modulus. Within the framework of the Hertz contact theory, E^* is determined as a combination of elastic moduli E_i , E_s and Poisson's ratios ν_i , ν_s for indenter (with index i) and sample (index s) through relation (2)

$$\frac{1}{E^*} = \frac{1 - \nu_i^2}{E_i} + \frac{1 - \nu_s^2}{E_s} \quad (2)$$

It follows from (2) that the basic relation for determination of the sample elastic modulus E_s is

$$E_s = \left(1 - \frac{E^*}{E_i} \right)^{-1} (1 - \nu_s^2) E^* \quad (3)$$

where $E_i^* = \frac{E_i}{1 - \nu_i^2}$ is the reduced elastic contact modulus of the indenter.

The basic relation for hardness value H is given as

$$H = \frac{P_{\max}}{A} \quad (4)$$

where P_{\max} is the peak force applied to the surface by indenter.

It could be seen that both relations (3) and (4) are based on determination of the

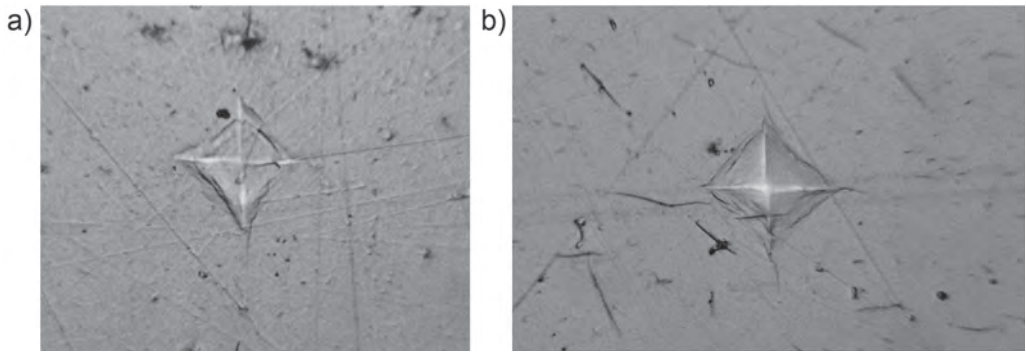


Fig. 3. Typical shapes of imprints after microhardness tests of the 'as received' coal samples: the coal #1 (a); the coal #2 (b)

contact are. A between the sample and the indenter. The aforementioned quantity is traditionally estimated by procedure described in [32, 33]. The estimations are based on the value of the contact depth. On the other hand, as it was noted in [26, 34], the approximations from [32, 33] do not take properly into account the plastic distortions of the sample surfaces and, consequently, the procedure introduces additional inaccuracy of measurements of hardness and elastic moduli during indentation. Therefore, that the mechanical characteristics obtained have to be treated rather carefully because the contact area between the indenter and the sample is measured with inaccuracies.

Results and discussion

Features of microscale fracturing of selected coals

As it has been already mentioned [17], the coals samples have different characteristic shapes of imprints. Namely, the coal #1 selected from non-hazardous pack, has rather 'plastic' imprints with lack of fracturing out of the contact zone (see Fig. 3, a), whereas the coal sample #2 originated from the outburst-prone pack shows rather brittle behavior with a large number of fractures either inside and coming outside the contact region (see Fig. 3, b).

Heterogeneity of maps of nanoscale hardness

First, it is worth mentioning that the average diagonal of the imprints after microindentation was about 32 μm , and the side of the zone where the nanoindentation grid tests were performed was 50 μm . This allows to conclude that the sizes of the contact region of microindentation and the zone of grid nanoindentation were of the same order of magnitude. Therefore, nanoindentation tests and mapping of their outcomes enabled us to investigate the heterogeneity of the distributions of hardness values across a region comparable with the plastic imprint obtained in the microhardness tests.

Fig. 4 shows typical maps of hardness values distribution across the selected regions. It could be seen that the average hardness of the coal #2 from a potentially outburst-prone pack is lower than the average hardness of the coal #1. Standard deviations for both coals are similar indicating the similarity of hardness values distribution heterogeneity (see Fig. 4, a, c).

Dimethylformamide treatment of these coals led to the following. Average hardness values have become similar for both of the samples, with their standard deviation decrease for the coal #2. On the other hand, maps of hardness distribution are rather similar for the both coals.

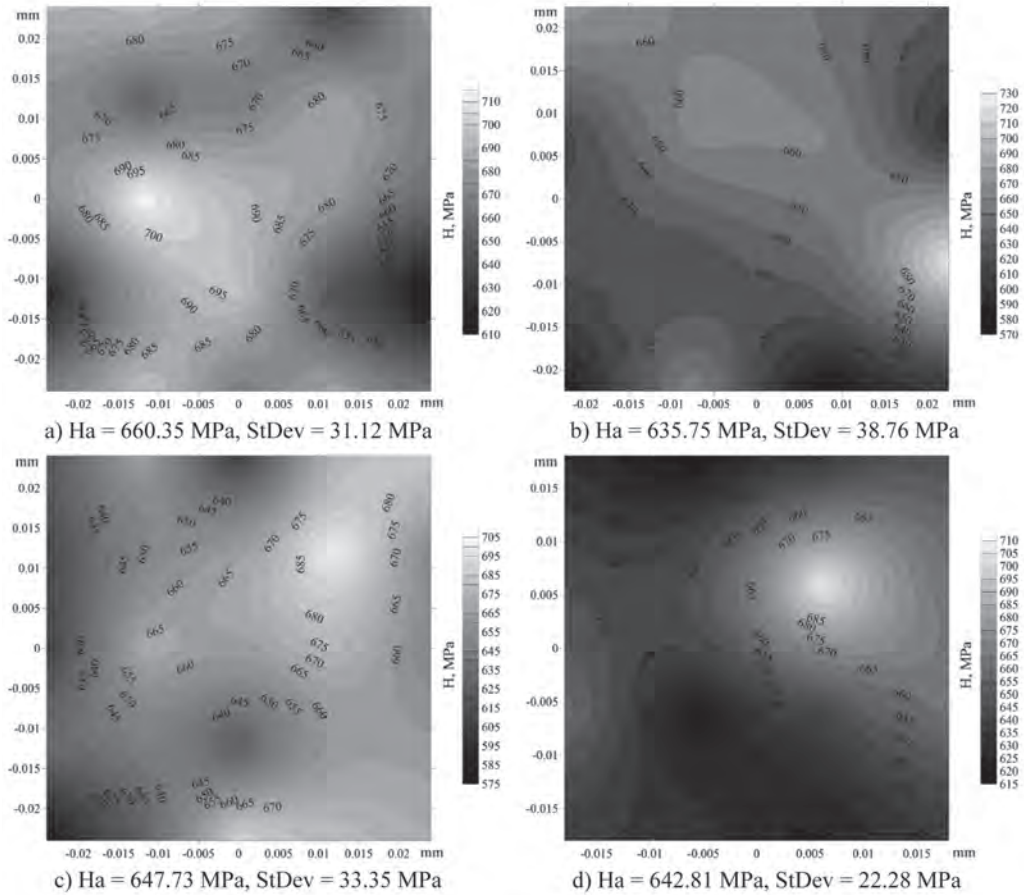


Fig. 4. Hardness mapping: the 'as received' coal #1 (a); the sorption treated coal #1 (b); the 'as received' coal #2 (c); the sorption treated coal #2 (H_a is the average hardness, StDev is the standard deviation of hardness) (d)

The above outcomes lead to the conclusion that the nanoscale hardness could not be used as an informative parameter for characterization of coals vitrinite brittleness or be employed for prediction of the fine dust formation.

Heterogeneity of the elastic modulus distribution extracted from nanoindentation tests

As it has been mentioned above, elastic modulus is a measure of materials stiffness. Hence, it follows from Fig. 5, a, c, that the coal #1 has a stiffer vitrinite structure than the coal from an outburst-prone pack

(see the captions to Fig. 5, a, c). Moreover, the values of the elastic modulus have more homogenous distribution within the coal #1 in comparison with the distribution within the coal #2 (see the standard deviations and images in Fig. 5, a, c). In addition, it follows from Fig. 5, c, that the coal #2 contains relatively large inclusions having small stiffness (the large soft inclusions) and small inclusions having higher range values of elastic modulus (the small hard inclusions).

After sorption treatment, the coal #1 became in average less stiff, whereas the coal #2 became in average stiffer (Fig. 5 b, d).

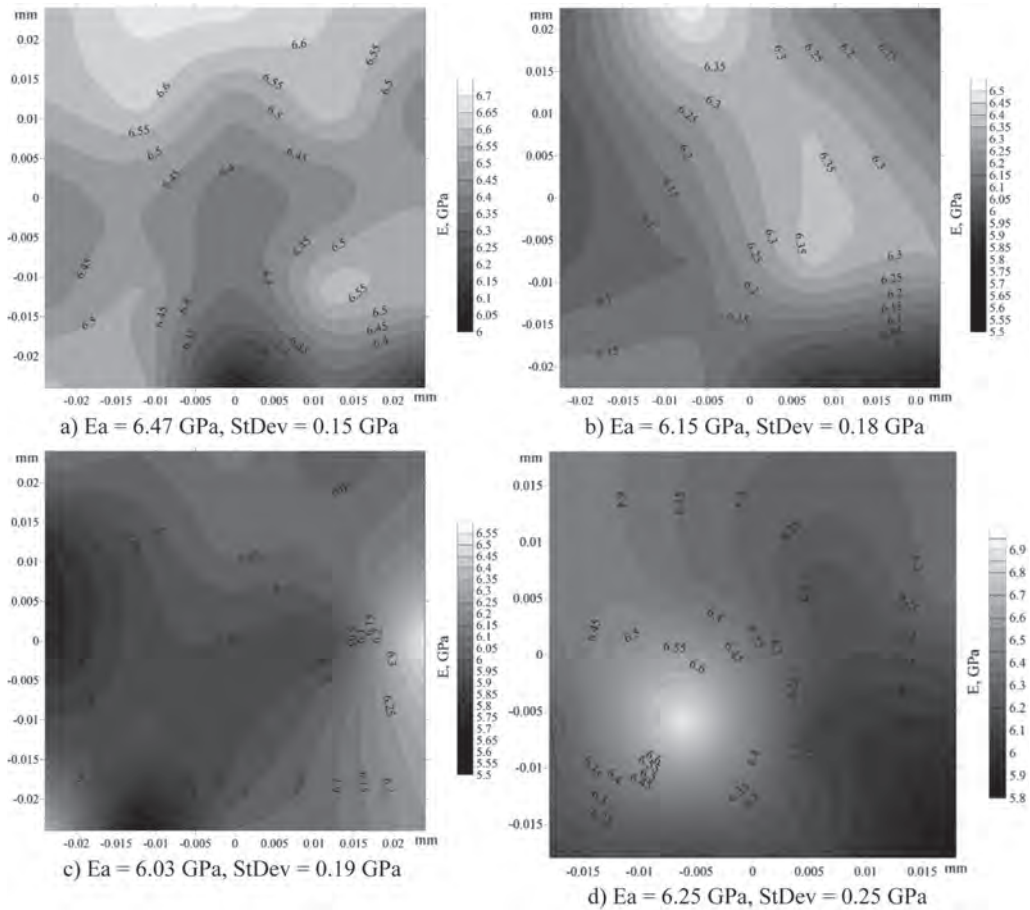


Fig. 5. Elastic modulus mapping: the ‘as received’ coal #1 (a); the sorption treated coal #1 (b); the ‘as received’ coal #2 (c); the sorption treated coal #2 treated (E_a – average elastic modulus, $StDev$ – standard deviation of elastic modulus) (d)

Standard deviation of elastic modulus has increased in both cases. Therefore, heterogeneity of elastic modulus distribution has also increased, but in case of the coal #2 this growth is more pronounced. In case of the coal #1, this distribution has revealed its ‘structural’ character, i.e. there appeared almost rectangular clusters of stiffer and less stiff regions. This distribution reflects in some sense the shapes of fractures that have been found at its surface after dimethylformamide treatment (see Fig. 1, a). On the contrary, coal #2 after sorption treatment appears not to have any ‘structural’ heterogeneities distri-

bution for the elastic modulus. Their sizes have remained at the same level as for the ‘as received’ sample (see Fig. 5 c, d). Lack of any pattern in elastic modulus distribution is in a good correlation with features of the coal #2 sorption-induced destruction of the surface (see Fig. 1, b). These conclusions are in agreement with our previous results presented in [17].

There is a plausible explanation of the above observations that after the sorption treatment, the residual stresses have been partially discharged within both of the coals. Hence, the tests of these samples reveal the differences in internal heteroge-

neity of mechanical properties that are not affected by internal residual stresses.

It is natural to state that the material having inclusions with equal share of high and low stiffness is more prone to destruction than the one having lower range of the stiffness distribution. Therefore, according to our observations on both ‘as received’ and sorption treated coals, the samples extracted from an outburst-prone pack are more brittle in comparison with the coal #1 having rather homogenous vitrinite structure. The latter is in a good correlation with the characteristic shapes of imprints obtained at these coals by microindentation (see Fig. 3).

Parameter R_w distribution heterogeneity

It should be reminded again that parameter R_w is closely connected to coals propensity to degradation under mechanical loading (nanoindentation). The higher this quantity, the larger the ductility and brittleness and, therefore one can assume that a larger amount of the crushed material (the fine powder) could be formed in the contact zone under the indenter. The results of this parameter mapping for the coals #1 and #2 are shown in Fig. 6.

The average values of R_w are similar for both coals, whereas their standard deviations are different, it is larger for coal #2 (from the outburst-prone pack) that

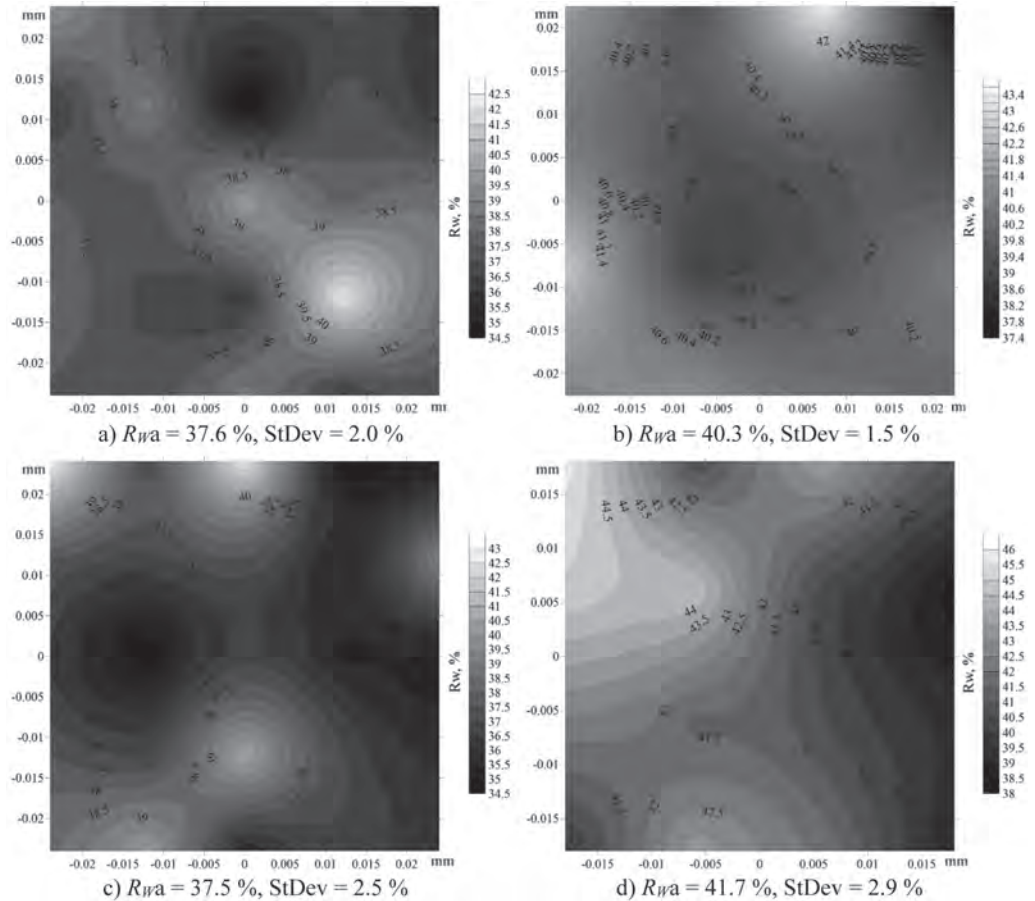


Fig. 6. R_w parameter mapping: a) coal #1 as received (a); coal #1 treated (b); coal #2 as received (c); coal #2 treated (R_{wa} – average elastic modulus, StDev – standard deviation of R_w) (d)

indicates its higher heterogeneity degree.

It is worth mentioning that in comparison with the coal #2, the coal #1 has rather low amount of inclusions that are more prone to destruction, whereas the 'stronger' regions are wider, while there exists an equal share of stronger and less strong inclusions within the coal #2. This is again in a good correlation with the characteristic surface damages of these coals after dimethylformamide treatment (see Fig. 1).

Dimethylformamide treatment of the selected coals led to the following changes. The coal #1 average R_w value showed a significant growth indicating an increase of its ductility, whereas the standard deviation drastically decreased showing the homogeneity of its distribution (see Fig. 6, b). The coal #2 demonstrated also the growth of R_w average value, but its distribution has become even more heterogenous (see Fig. 6, d). The less strong inclusions have also increased in size, whereas the stronger ones became smaller.

The observations on R_w parameter distribution for the considered coals indicate the differences between their propensity to destruction and formation of fine powder (dust).

Connections between heterogeneity of mechanical properties distribution at nanoscale and microhardness imprints shapes after sorption treatment

All the observations shown above now allow us to explain some features of fracturing of the dimethylformamide treated coals after microhardness tests. Fig. 7 shows the typical shapes of imprints.

It could be seen that after dimethylformamide treatment, shapes of the coal #1 imprints have not changed significantly, only few radial cracks coming out of the imprint corners were formed. On the other hand, the coal #2 imprints after sorption treatment have drastically changed, namely, having internal damage, long radial cracks from the imprint corners and lateral cracks neighboring the sides of the contact region.

Increase of heterogeneity of stiffness and R_w values distribution at nanoscale for the coal #2 after sorption treatment has led to significant damage within the contact zone and the neighbouring region.

Dimethylformamide treatment allowed to reveal the following. The coal from the outburst-prone pack is characterized by very high natural heterogeneity of its mechanical properties measured at nanoscale, leading to drastic damage of its surface

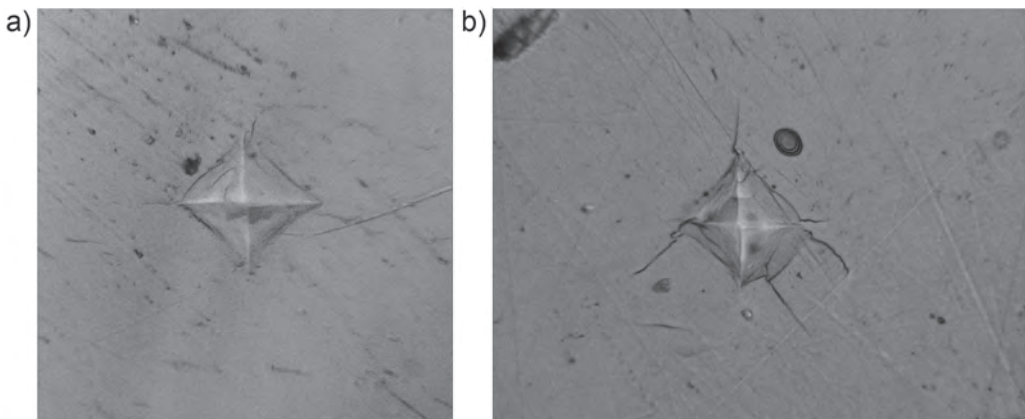


Fig. 7. Typical shapes of imprints after microhardness tests of coal samples after sorption treatment: the coal #1 (a); the coal #2 (b)

after microhardness tests. Coal from the non-hazardous pack is found to have rather homogenous distribution of R_w parameter and 'structural' distribution of its stiffness (elastic modulus) leading to formation of only a few radial fractures after microindentation.

It could be concluded that dimethylformamide treatment of coals having similar origin, type and rank, however having different propensity to instantaneous outbursts enabled us to conduct a deeper analysis of the heterogeneity of their mechanical properties at nanoscale. This may be explained that such processing of coals led to partial discharge of the residual stresses that exist in the coals. The latter revealed the natural (structurally-induced) differences between their internal mechanical properties.

Conclusions

In accordance with the investigation shown in the article, the following conclusions could be made.

1. It has been demonstrated that the ability of coals to create fine dust during mechanical interactions with hard instruments may be correlated with the heterogeneity of distributions of their mechanical properties (the local elastic modulus and hardness) obtained from nanoscale indentation tests. The maps of the distributions may be obtained by analysis of the automatic grid indentation of polished coal surfaces. In addition, mapping of parameter R_w defining the share of work that was introduced characterizing the irreversible changes in the material structure in the total loading work. Regarding the brittleness of coals, this parameter could be treated to be closely connected with the degradation (destruction) at indentation.

2. Experiments were performed at coals from hazardous with respect to sudden coal and gas outbursts and non-haz-

ardous packs of one coal seam. The tested samples included 'as received' coals and those after sorption treatment by dimethylformamide. The latter treatment leads to partial discharge of the internal stresses existing in the coal samples and reveal the actual nanoscale heterogeneity of mechanical properties that is not affected by residual stresses.

3. Hardness values distribution appeared to be similar for both coals, and for both 'as received' and 'sorption treated by dimethylformamide' samples. These results confirmed our earlier statement that the coal nanoscale hardness is not an informative parameter for characterization of coals propensity to destruction.

4. The coal from potentially outburst-prone pack is characterized by relatively higher heterogeneity of elastic modulus (stiffness) distribution in comparison with the coal from non-hazardous pack. Higher heterogeneity of such a value could be a reason to formation of multiple cracks after microhardness tests. Whereas, for coal with lower heterogeneity of elastic modulus distribution, the resulting imprints do not appear to have fractures.

5. The observations on R_w parameter distribution for the considered coals clearly indicate the differences between their propensity to destruction and formation of fine powder (dust). Coal from the non-hazardous pack has rather low amount of inclusions that are more prone to irreversible changes of the structure after loading, whereas the 'stronger' regions are wider. Coal originated from the hazardous pack is characterized by an equal share of stronger and less strong inclusions. This is in a good correlation with the characteristic surface damages of these coals after dimethylformamide treatment.

6. Dimethylformamide treatment allowed to reveal the natural (structurally-based) heterogeneity of coals mechanical properties at nanoscale. This made it

possible to find the natural diversity of the mechanical properties of two coals having similar origin, type and rank but different in their proneness to instantaneous outbursts.

Thus, the results presented above enabled us to conclude that outburst-prone and non-hazardous coals as well as the coals prone to creation of a large amount of dust particles and the coals that do not

have such a property, may be qualitatively distinguished by the heterogeneity of the coal mechanical properties evaluated from nanindentation tests. However, the models for quantitative calculations of the dust particles distributions should be based on statistical approaches and employment of properties obtained for the representative volume of a particular coal pack.

СПИСОК ЛИТЕРАТУРЫ

1. *Rout T.K., Masto R.E., Padhy P.K., George J., Ram L.C., Maity S.* Dust fall and elemental flux in a coal mining area // *Journal of Geochemical Exploration*, 2014. Vol. 144, no PC, pp. 443–455. DOI: 10.1016/j.gexplo.2014.04.003.

2. *Tang Z., Chai M., Cheng J., Jin J., Yang Y., Nie Z., Huang Q., Li Y.* Contamination and health risks of heavy metals in street dust from a coal-mining city in eastern China // *Ecotoxicology and Environmental Safety*, 2017. Vol. 138, pp. 83–91. DOI: 10.1016/j.ecoenv.2016.11.003.

3. *Shepherd J., Rixon L.K., Griffiths L.* Outbursts and geological structures in coal mines: A review // *International Journal of Rock Mechanics and Mining Sciences* and, 1981. Vol. 18, no 4, pp. 267–283. DOI: 10.1016/0148-9062(81)91192-X.

4. *Lama R.D., Bodziony J.* Management of outburst in underground coal mines // *International Journal of Coal Geology*, 1998. Vol. 35, no 1–4, pp. 83–115. DOI: 10.1016/S0166-5162(97)00037-2.

5. *Fedorova G.G., Sidorov I.N., Afanas'ev K.M.* Dispersion of coal in a gaseous medium under the influence of physicochemical processes, and methods of dust suppression // *Soviet Mining Science*, 1974. Vol. 10, no 4, pp. 498–503. DOI: 10.1007/BF02501444.

6. *Johann-Essex V., Keles C., Rezaee M., Scaggs-Witte M., Sarver E.* Respirable coal mine dust characteristics in samples collected in central and northern Appalachia // *International Journal of Coal Geology*, 2017. Vol. 182, no March, pp. 85–93. DOI: 10.1016/j.coal.2017.09.010.

7. *Organiscak J.A., Page S.J.* Airborne Dust Liberation During Coal Crushing // *Coal Preparation*, 2000. Vol. 21, no 5–6, pp. 423–453. DOI: 10.1080/07349340108945630.

8. *An F.H., Cheng Y.P.* An explanation of large-scale coal and gas outbursts in underground coal mines: The effect of low-permeability zones on abnormally abundant gas // *Natural Hazards and Earth System Sciences*, 2014. Vol. 14, no 8, pp. 2125–2132. DOI: 10.5194/nhess-14-2125-2014.

9. *Fisne A., Esen O.* Coal and gas outburst hazard in Zonguldak Coal Basin of Turkey, and association with geological parameters // *Natural Hazards*, 2014. Vol. 74, no 3, pp. 1363–1390. DOI: 10.1007/s11069-014-1246-9.

10. *Ding Y., Dou L., Cai W., Chen J., Kong Y., Su Z., Li Z.* Signal characteristics of coal and rock dynamics with micro-seismic monitoring technique // *International Journal of Mining Science and Technology*, 2016. Vol. 26, no 4, pp. 683–690. DOI: 10.1016/j.ijmst.2016.05.022.

11. *Wang S., Elsworth D., Liu J.* Rapid decompression and desorption induced energetic failure in coal // *Journal of Rock Mechanics and Geotechnical Engineering*, 2015. Vol. 7, no 3, pp. 345–350. DOI: 10.1016/J.JRMGE.2015.01.004.

12. *Wen Z., Wang X., Tan Y., Zhang H., Huang W., Li Q.* A Study of Rockburst Hazard Evaluation Method in Coal Mine // *Shock and Vibration*, 2016. Vol. 2016, pp. 1–9. DOI: 10.1155/2016/8740868.

13. *Li X., Wang C., Zhao C., Yang H.* The propagation speed of the cracks in coal body containing gas // *Safety Science*, 2012. Vol. 50, no 4, pp. 914–917. DOI: 10.1016/j.ssci.2011.08.004.

14. *Beamish B.B., Crosdale P.J.* Instantaneous outbursts in underground coal mines: an overview and association with coal type // *International Journal of Coal Geology*, 1998. Vol. 35, no 1–4, pp. 27–55. DOI: 10.1016/S0166-5162(97)00036-0.

15. *Molchanov O., Rudakov D., Soboliev V., Kamchatnyi O.* Destabilization of the hard coal microstructure by a weak electric field // E3S Web of Conferences, 2018. Vol. 60, pp. 00023. DOI: 10.1051/e3sconf/20186000023.
16. *Bobin V.A., Malinnikova O.N., Odintsev V.N., Trofimov V.A.* Analysis of the connection between the microstructure and gas-dynamic fracture susceptibility in coal // Gornyi Zhurnal, 2017, pp. 22–27. DOI: 10.17580/gzh.2017.11.04.
17. *Эпштейн С.А., Коссович Е.Л., Просина В.А., Добрякова Н.Н.* Особенности сорбционного разупрочнения углей из потенциально выбросоопасных и неопасных пачек // Горный журнал. — 2018. — № 12. — С. 18–22. DOI: 10.17580/gzh.2018.12.04.
18. *Sergejev F., Kimmari E., Viljus M.* Residual Stresses in TiC-based Cermets Measured by Indentation // Procedia Engineering, 2011. Vol. 10, pp. 2873–2881. DOI: 10.1016/j.proeng.2011.04.477.
19. *Ватульян А.О., Ляпин А.А., Коссович Е.Л.* Исследование упругопластических свойств угольных пород на основе метода индентирования // Известия Саратовского университета. Новая серия. Серия: Математика. Механика. Информатика. — 2018. — Т. 18. — вып. 4. — С. 412–420. DOI: 10.18500/1816-9791-2018-18-4-412-420.
20. *ASTM D7708-14*, Standard Test Method for Microscopical Determination of the Reflectance of Vitrinite Dispersed in Sedimentary Rocks // West Conshohocken, PA, 2014, www.astm.org: ASTM International. DOI: 10.1520/D7708-14.
21. *Коссович Е.Л., Эпштейн С.А., Шкуратник В.Л., Минин М.Г.* Перспективы и проблемы использования современной техники микро- и наноиндентирования для диагностики механических свойств углей // Горный журнал. — 2017. — № 12. — С. 25–30. DOI: 10.17580/gzh.2017.12.05.
22. *Kossovich E., Epshtein S., Dobryakova N., Minin M., Gavrilova D.* Mechanical Properties of Thin Films of Coals by Nanoindentation // Physical and Mathematical Modeling of Processes in Geomedia, Moscow: IPMech RAS, 2018, pp. 45–50. DOI: 10.1007/978-3-319-77788-7_6.
23. *ГОСТ 21206-75* Угли каменные и антрацит. Метод определения микротвердости и микрохрупкости. — М.: Издательство стандартов, 1977.
24. *ASTM E384*: Standard Test Method for Microindentation Hardness of Materials // Annual Book of ASTM Standards, PA: ASTM International, West Conshohocken, 2016. 1-42 p. DOI: 10.1520/E0384-10.2.
25. *Хрущов М.М., Беркович Е.С.* Приборы ПМТ-2 и ПМТ-3 для испытания на микротвердость. — М.: Изд-во АН СССР, 1950. — 66 с.
26. *Kossovich E.L., Borodich F.M., Epshtein S.A., Galanov B.A., Minin M.G., Prosina V.A.* Mechanical, structural and scaling properties of coals: depth-sensing indentation studies // Applied Physics A, 2019. Vol. 125, no 3, pp. 195. DOI: 10.1007/s00339-018-2282-1.
27. *Sakai M.* Energy principle of the indentation-induced inelastic surface deformation and hardness of brittle materials // Acta Metallurgica Et Materialia, 1993. Vol. 41, no 6, pp. 1751–1758. DOI: 10.1016/0956-7151(93)90194-W.
28. *Argatov I.I., Borodich F.M., Epshtein S.A., Kossovich E.L.* Contact stiffness depth-sensing indentation: Understanding of material properties of thin films attached to substrates // Mechanics of Materials, 2017. Vol. 114, pp. 172–179. DOI: 10.1016/j.mechmat.2017.08.009.
29. *Baumgart F.* Stiffness – an unknown world of mechanical science? // Injury, 2000. Vol. 31, pp. S-B14-S-B23. DOI: 10.1016/S0020-1383(00)80040-6.
30. *Borodich F.M.* The Hertz-Type and Adhesive Contact Problems for Depth-Sensing Indentation // Advances in Applied Mechanics, 2014. Vol. 47, pp. 225–366. DOI: 10.1016/B978-0-12-800130-1.00003-5.
31. *Булычев С.И., Алехин В.П., Шоршоров М.Х., Терновский А.П., Шнырев Г.Д., Шнырев Г.Д.* Определение модуля Юнга по диаграмме вдавливания индентора // Заводская лаборатория. — 1975. — Т. 41. — № 9. — с. 1137-1140.
32. *Oliver W.C., Pharr G.M.* An improved technique for determining hardness and elastic modulus using load and displacement sensing indentation experiments // Journal of Materials Research, 1992. Vol. 7, no 06, pp. 1564–1583. DOI: 10.1557/JMR.1992.1564.
33. *Oliver W.C., Pharr G.M.* Measurement of hardness and elastic modulus by instrumented indentation: Advances in understanding and refinements to methodology // Journal of Materials Research, 2004. Vol. 19, no 01, pp. 3–20. DOI: 10.1557/jmr.2004.19.1.3.

34. Галанов Б. А., Дуб С. Н. Критические комментарии к методике Оливера-Фара для измерения твердости и упругого модуля посредством инструментального индентирования и уточнение ее базисных соотношений // Сверхтвердые материалы. — 2017. — Т. 39. — № 6. — С. 373–389. DOI: 10.3103/S1063457617060016. **PLAB**

REFERENCES

1. Rout T. K., Masto R. E., Padhy P. K., George J., Ram L. C., Maity S. Dust fall and elemental flux in a coal mining area. *Journal of Geochemical Exploration*, 2014. Vol. 144, no PC, pp. 443–455. DOI: 10.1016/j.gexplo.2014.04.003.
2. Tang Z., Chai M., Cheng J., Jin J., Yang Y., Nie Z., Huang Q., Li Y. Contamination and health risks of heavy metals in street dust from a coal-mining city in eastern China. *Ecotoxicology and Environmental Safety*, 2017. Vol. 138, pp. 83–91. DOI: 10.1016/j.ecoenv.2016.11.003.
3. Shepherd J., Rixon L. K., Griffiths L. Outbursts and geological structures in coal mines. A review. *International Journal of Rock Mechanics and Mining Sciences and*, 1981. Vol. 18, no 4, pp. 267–283. DOI: 10.1016/0148-9062(81)91192-X.
4. Lama R. D., Bodziony J. Management of outburst in underground coal mines. *International Journal of Coal Geology*, 1998. Vol. 35, no 1–4, pp. 83–115. DOI: 10.1016/S0166-5162(97)00037-2.
5. Fedorova G. G., Sidorov I. N., Afanas'ev K. M. Dispersion of coal in a gaseous medium under the influence of physicochemical processes, and methods of dust suppression. *Soviet Mining Science*, 1974. Vol. 10, no 4, pp. 498–503. DOI: 10.1007/BF02501444.
6. Johann-Essex V., Keles C., Rezaee M., Scaggs-Witte M., Sarver E. Respirable coal mine dust characteristics in samples collected in central and northern Appalachia. *International Journal of Coal Geology*, 2017. Vol. 182, no March, pp. 85–93. DOI: 10.1016/j.coal.2017.09.010.
7. Organiscak J. A., Page S. J. Airborne Dust Liberation During Coal Crushing. *Coal Preparation*, 2000. Vol. 21, no 5–6, pp. 423–453. DOI: 10.1080/07349340108945630.
8. An F. H., Cheng Y. P. An explanation of large-scale coal and gas outbursts in underground coal mines: The effect of low-permeability zones on abnormally abundant gas. *Natural Hazards and Earth System Sciences*, 2014. Vol. 14, no 8, pp. 2125–2132. DOI: 10.5194/nhess-14-2125-2014.
9. Fisne A., Esen O. Coal and gas outburst hazard in Zonguldak Coal Basin of Turkey, and association with geological parameters. *Natural Hazards*, 2014. Vol. 74, no 3, pp. 1363–1390. DOI: 10.1007/s11069-014-1246-9.
10. Ding Y., Dou L., Cai W., Chen J., Kong Y., Su Z., Li Z. Signal characteristics of coal and rock dynamics with micro-seismic monitoring technique. *International Journal of Mining Science and Technology*, 2016. Vol. 26, no 4, pp. 683–690. DOI: 10.1016/j.ijmst.2016.05.022.
11. Wang S., Elsworth D., Liu J. Rapid decompression and desorption induced energetic failure in coal. *Journal of Rock Mechanics and Geotechnical Engineering*, 2015. Vol. 7, no 3, pp. 345–350. DOI: 10.1016/J.JRMGE.2015.01.004.
12. Wen Z., Wang X., Tan Y., Zhang H., Huang W., Li Q. A Study of Rockburst Hazard Evaluation Method in Coal Mine. *Shock and Vibration*, 2016. Vol. 2016, pp. 1–9. DOI: 10.1155/2016/8740868.
13. Li X., Wang C., Zhao C., Yang H. The propagation speed of the cracks in coal body containing gas. *Safety Science*, 2012. Vol. 50, no 4, pp. 914–917. DOI: 10.1016/j.ssci.2011.08.004.
14. Beamish B. B., Crosdale P. J. Instantaneous outbursts in underground coal mines: an overview and association with coal type. *International Journal of Coal Geology*, 1998. Vol. 35, no 1–4, pp. 27–55. DOI: 10.1016/S0166-5162(97)00036-0.
15. Molchanov O., Rudakov D., Soboliev V., Kamchatnyi O. Destabilization of the hard coal microstructure by a weak electric field. *E3S Web of Conferences*, 2018. Vol. 60, pp. 00023. DOI: 10.1051/e3sconf/20186000023.
16. Bobin V. A., Malinnikova O. N., Odintsev V. N., Trofimov V. A. Analysis of the connection between the microstructure and gas-dynamic fracture susceptibility in coal. *Gornyi Zhurnal*, 2017, pp. 22–27. DOI: 10.17580/gzh.2017.11.04.
17. Epshtein S. A., Kossovich E. L., Prosina V. A., Dobryakova N. N. Features of sorption-induced strength degradation of coals originated from potentially prone to outburst and non-hazardous packs. *Gornyi Zhurnal*, 2018, no 12, pp. 18–22. DOI: 10.17580/gzh.2018.12.04.

18. Sergejev F., Kimmari E., Viljus M. Residual Stresses in TiC-based Cermets Measured by Indentation. *Procedia Engineering*, 2011. Vol. 10, pp. 2873–2881. DOI: 10.1016/j.proeng.2011.04.477.
19. Vatulyan A.O., Lyapin A.A., Kossovich E.L. Studying of Elastoplastic Properties of Coal Specimens Using Indentation Technique. *Izv. Saratov Univ. (N. S.), Ser. Math. Mech. Inform.*, 2018. Vol. 18, no 4, pp. 412–420. DOI: 10.18500/1816-9791-2018-18-4-412-420.
20. ASTM D7708-14, *Standard Test Method for Microscopical Determination of the Reflectance of Vitrinite Dispersed in Sedimentary Rocks*. West Conshohocken, PA, 2014, www.astm.org: ASTM International. DOI: 10.1520/D7708-14.
21. Kossovich E.L., Epshtein S.A., Shkuratnik V.L., Minin M.G. Perspectives and problems of modern depth-sensing indentation techniques application for diagnostics of coals mechanical properties. *Gornyi Zhurnal*, 2017. Vol. 2017, no 12, pp. 25–30. DOI: 10.17580/gzh.2017.12.05.
22. Kossovich E., Epshtein S., Dobryakova N., Minin M., Gavrilova D. Mechanical Properties of Thin Films of Coals by Nanoindentation. *Physical and Mathematical Modeling of Processes in Geomedia*, Moscow: IPMech RAS, 2018, pp. 45–50. DOI: 10.1007/978-3-319-77788-7_6.
23. GOST 21206-75 Coals and anthracite. Determination method for microhardness and microbrittleness. Moscow: Standards publishing, 1977. Russian p.
24. ASTM. *ASTM E384: Standard Test Method for Microindentation Hardness of Materials*. Annual Book of ASTM Standards, PA: ASTM International, West Conshohocken, 2016. 1-42 p. DOI: 10.1520/E0384-10.2.
25. Khrushchov M.M., Berkovich E.S. *Devices PMT-2 and PMT-3 for microhardness testing*. Moscow, Izdatelstvo AN USSR, 1950. 66 p.
26. Kossovich E.L., Borodich F.M., Epshtein S.A., Galanov B.A., Minin M.G., Prosina V.A. Mechanical, structural and scaling properties of coals: depth-sensing indentation studies. *Applied Physics A*, 2019. Vol. 125, no 3, pp. 195. DOI: 10.1007/s00339-018-2282-1.
27. Sakai M. Energy principle of the indentation-induced inelastic surface deformation and hardness of brittle materials. *Acta Metallurgica Et Materialia*, 1993. Vol. 41, no 6, pp. 1751–1758. DOI: 10.1016/0956-7151(93)90194-W.
28. Argatov I.I., Borodich F.M., Epshtein S.A., Kossovich E.L. Contact stiffness depth-sensing indentation: Understanding of material properties of thin films attached to substrates. *Mechanics of Materials*, 2017. Vol. 114, pp. 172–179. DOI: 10.1016/j.mechmat.2017.08.009.
29. Baumgart F. Stiffness – an unknown world of mechanical science?. *Injury*, 2000. Vol. 31, pp. S-B14-S-B23. DOI: 10.1016/S0020-1383(00)80040-6.
30. Borodich F.M. The Hertz-Type and Adhesive Contact Problems for Depth-Sensing Indentation. *Advances in Applied Mechanics*, 2014. Vol. 47, pp. 225–366. DOI: 10.1016/B978-0-12-800130-1.00003-5.
31. Bulychev S.I., Alekhin V.P., Shorshorov M.K., Ternovskij A.P., Shnyrev G.D. Determination of Young modulus by the hardness indentation diagram. *Zavodskaya Laboratoriya*, 1975. Vol. 41, no 9, pp. 1137–1140.
32. Oliver W.C., Pharr G.M. An improved technique for determining hardness and elastic modulus using load and displacement sensing indentation experiments. *Journal of Materials Research*, 1992. Vol. 7, no 06, pp. 1564–1583. DOI: 10.1557/JMR.1992.1564.
33. Oliver W.C., Pharr G.M. Measurement of hardness and elastic modulus by instrumented indentation: Advances in understanding and refinements to methodology. *Journal of Materials Research*, 2004. Vol. 19, no 01, pp. 3–20. DOI: 10.1557/jmr.2004.19.1.3.
34. Galanov B.A., Dub S.N. Critical comments to the Oliver–Pharr measurement technique of hardness and elastic modulus by instrumented indentations and refinement of its basic relations. *Journal of Superhard Materials*, 2017. Vol. 39, no 6, pp. 373–389. DOI: 10.3103/S1063457617060016.

ИНФОРМАЦИЯ ОБ АВТОРАХ

Коссович Елена Леонидовна¹ — кандидат физико-математических наук, старший научный сотрудник, e-mail: e.kossovich@misis.ru,

Эпштейн Светлана Абрамовна¹ — доктор технических наук,

старший научный сотрудник, зав. лабораторией, e-mail: apshstein@yandex.ru,

Бородич Федор Михайлович — доктор физико-математических наук, профессор, институт Инженерии, Университет Кардиффа, Кардифф, Великобритания,
Добрякова Надежда Николаевна¹ — кандидат технических наук, ведущий инженер,
Просина Вера Алексеевна¹ — инженер,
¹ Научно-учебная испытательная лаборатория «Физико-химии углей», НИТУ «МИСиС».
Для контактов: Коссович Е. Л., e-mail: e.kossovich@misis.ru.

INFORMATION ABOUT THE AUTHORS

E.L. Kossovich¹, Ph.D., senior researcher, e-mail: e.kossovich@misis.ru,
S.A. Epshtein¹, D.Sci. (Engineering), Head of Laboratory, e-mail: apshtein@yandex.ru,
F.M. Borodich, D.Sci. (Physics and Mathematics), Professor,
School of Engineering, Cardiff University, Cardiff, UK,
N.N. Dobryakova¹, Ph.D. (Engineering), Leading Engineer,
V.A. Prosina¹, Engineer,
¹ Scientific and Training Laboratory of Physics and Chemistry of Coals,
National University of Science and Technology «MISiS», 119049, Moscow, Russia.
Corresponding author: E.L. Kossovich, e-mail: e.kossovich@misis.ru.



РУКОПИСИ, ДЕПОНИРОВАННЫЕ В ИЗДАТЕЛЬСТВЕ «ГОРНАЯ КНИГА»

МОДЕЛИРОВАНИЕ УСТРОЙСТВА ПЛАВНОГО ПУСКА АСИНХРОННОГО ДВИГАТЕЛЯ (№ 1181/05–19 от 27.03.2019; 17 с.)

Дмитриева Валерия Валерьевна¹ — кандидат технических наук, доцент,
Гаврилов Алексей Анатольевич¹ — студент, e-mail: alexgavrilov9614@gmail.com,
¹ РГУ Нефти и газа (НИУ) им. И.М. Губкина.

Асинхронные электрические двигатели с короткозамкнутым ротором получили широкое распространение. В промышленных электродвигателях пусковые токи могут достигать очень высоких значений, что приводит к просадкам напряжения в сети, перегрузкам подстанций и электропроводки. Для управления асинхронными электродвигателями обычно используется устройство плавного пуска (УПП). Оно объединяет функции плавного пуска и торможения, защиты механизмов и электродвигателей. Разработаны модели всех элементов, входящих в УПП. Получена полная модель тиристорного регулятора напряжения с асинхронным двигателем. В программе Simulink проведено моделирование, полученные результаты подтверждают адекватность модели. Результаты моделирования демонстрируют, что устройство плавного пуска асинхронного двигателя уменьшает пусковые токи, устраняет рывки в механических приводах, что, в конечном итоге, повышает срок службы электродвигателя.

Ключевые слова: асинхронный двигатель, устройство плавного пуска, тиристор, система импульсно-фазного управления, компьютерное моделирование, Simulink.

MODELING OF SOFT STARTER FOR ASYNCHRONOUS MOTOR

V.V. Dmitrieva¹, Candidate of Technical Sciences, Assistant Professor, e-mail: dm-valeriya@yandex.ru,
A.A. Gavrilov¹, Student, e-mail: alexgavrilov9614@gmail.com,
¹ Gubkin Russian State University of Oil and Gas, 119991, Moscow, Russia.

Asynchronous electric motors with squirrel cage rotor are widely used. In industrial electric motors, starting currents can reach very high values, which leads to voltage subsidence in the network, overloads of substations and electrical wiring. A soft starter is commonly used to control asynchronous motors. This device combines the functions of soft start and braking, protection mechanisms and motors. The article develops the model of all the elements included in the NPRM. By combining them, as shown in the figure, a complete model of the thyristor voltage regulator with an asynchronous motor is obtained. Simulink conducted a simulation, the results confirm the adequacy of the model. The simulation results demonstrate that the asynchronous motor soft-start device reduces starting currents, eliminates jerks in mechanical drives, which ultimately increases the service life of the electric motor.

Key word: asynchronous motor, soft-start device, thyristor, pulse-phase control system, computer simulation, Simulink.